



Record of heavy metals in Huguangyan Maar Lake sediments: Response to anthropogenic atmospheric pollution in Southern China



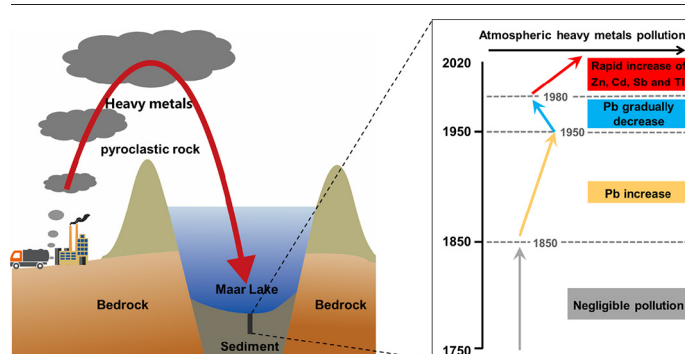
Hongchen Wu, Jingfu Wang^{*}, Jianyang Guo, Xiping Hu, Hongyun Bao, Jingan Chen^{*}

State Key Laboratory of Environmental Geochemistry, Institute of Geochemistry, Chinese Academy of Sciences, Guiyang 550081, PR China
University of Chinese Academy of Sciences, Beijing 100049, PR China

HIGHLIGHTS

- Heavy metals was measured in a well-dated sediment core from southern China.
- Zn, Cd, Sb, Tl are closely related to anthropogenic activities after 1980.
- Anthropogenic Pb began to increase since 1850 and reached a peak in 1950.
- Coal combustion is proposed as the main source of current atmospheric Pb.

GRAPHICAL ABSTRACT



ARTICLE INFO

Article history:

Received 29 December 2021
Received in revised form 18 March 2022
Accepted 22 March 2022
Available online 26 March 2022

Editor: Filip M.G. Tack

Keywords:

Lake sediments
Heavy metals
Lead isotopes
Atmospheric pollution
Southern China

ABSTRACT

The historical atmospheric heavy metal pollution of southern China over the past 200 years was explored by analyzing radiometric dating, heavy metals, and Pb isotopes from a sediment core in Huguangyan Maar Lake. Zn, Cd, Sb, Tl, and Pb in the lake are closely related to anthropogenic activities, while Cr and Ni are mainly derived from the weathering of basalt surrounding the lake. Atmospheric Zn, Cd, Sb, and Tl increased rapidly after 1980, consistent with the local industrial development. The increase of atmospheric Pb in southern China occurred earlier than in other regions of China, with the increase after 1850. War and the use of leaded gasoline were the main causes for the rapid increase in atmospheric Pb during 1910–1950. From 1950 to 2000, the input of Pb from anthropogenic activities decreased gradually due to the stable social environment. After 2000, atmospheric Pb continued to rise due to continued industrial development. The three-end-member model of Pb isotopes indicates that coal combustion is the main source of current atmospheric Pb. The proportion of Pb derived from vehicle exhaust emissions reached a peak in the 1960s, then gradually decreased and further reduced with the ban on leaded gasoline after 2000. These results are important in identifying the sources of atmospheric heavy metal pollution and in formulating pollution control strategies.

1. Introduction

Anthropogenic activities have significantly changed the atmospheric environment. The mining of mineral deposits, energy consumption, industrial production, and other activities, causes a large amount of toxic and

hazardous materials to be emitted into the atmosphere (Fayiga and Saha, 2016; Kribek et al., 2018; Lin et al., 2018; Pratte et al., 2018; Sondergaard et al., 2010; Zhang et al., 2016). Among these, heavy metals such as Cd and Pb are not required for normal physiological functions but cause significant harm to the environment and human health, while excessive intake of necessary trace elements such as Zn and Mn can also be toxic (Hall, 2002; Labonne et al., 2001; Nagajyoti et al., 2010). At present, the emission of atmospheric heavy metals can mainly be attributed to anthropogenic activities such as ore mining and smelting, vehicle exhaust, and

^{*} Corresponding authors at: State Key Laboratory of Environmental Geochemistry, Institute of Geochemistry, Chinese Academy of Sciences, Guiyang 550081, PR China.

E-mail addresses: wangjingfu@vip.skleg.cn (J. Wang), chenjingan@vip.skleg.cn (J. Chen).

industrial activities. These heavy metals can be transported to remote places through atmospheric circulation, settle onto surface environments through dry and wet deposition, and be recorded by environmental media (Huang et al., 2020; Omrani et al., 2017; Sierra-Hernandez et al., 2018; Wan et al., 2016).

As the world's factory, China has a rapidly developing industry. It accounts for approximately 30% of the total global industrial output, ranking it first in the world. However, China's rough development strategy has led to the problem of heavy metal pollution (Chan and Yao, 2008; Luo et al., 2011; Tian et al., 2015). Guangdong Province, in southern China, is one of the fastest growing regions, in terms of economic development in China (Liu et al., 2017; Wang et al., 2012). Atmospheric heavy metal pollution has a range of negative effects on the local environment, such as reducing water quality and causing damage to ecosystems. Previous studies on heavy metal pollution in Guangdong Province have mostly concentrated on environments such as soil, rivers, and coastal zones. In these environments, heavy metals have a variety of sources, thus it is difficult to distinguish atmospheric pollution source from other sources, while direct observations of atmospheric heavy metal concentrations usually have a short time scale (Chan and Yao, 2008; Li et al., 2016; Luo et al., 2011; Wong et al., 2002). Therefore, it is necessary to find other records to investigate the long-term historical variation in atmospheric heavy metals in this region. This is of great significance to understanding the processes of atmospheric heavy metal pollution, predicting future pollution trends, and formulating prevention and treatment strategies for atmospheric pollution.

Long-term studies on historical variation in air pollution usually use glacier ice or sediment cores from remote lakes (Lee et al., 2011; Rhodes et al., 2011; Wan et al., 2016; Wiklund et al., 2020). However, southern China has a low latitude and a dense population, so there are no glaciers or remote lakes. Fortunately, the Leizhou Peninsula in southern China experienced numerous periods of volcanic activity, which has formed several Maar lakes. Maar lakes are deep enclosed lakes with a stable sedimentary environment, meaning a continuous high-resolution sediment record can be obtained (Ortiz et al., 2013). The annular wall formed by volcanic eruption isolates the Maar lake from its external water body, so atmospheric deposition is an important input route for heavy metals. Therefore, sediments in Maar lakes reliably record the effects of natural processes and anthropogenic activities on the temporal trend of atmospheric heavy metal pollution (Ruiz-Fernandez et al., 2007).

In this study, a sediment core was collected from Huguangyan Maar Lake and its chronology was determined by ^{210}Pb and ^{137}Cs analysis. The

concentrations of several heavy metals (Pb, Cd, Zn, etc.) and major elements (Fe, Ca, Na, etc.) were analyzed, and lead isotopes (^{208}Pb , ^{207}Pb and ^{206}Pb) were measured. The main purpose of this study was to reconstruct the historical atmospheric heavy metal pollution in southern China over the past 200 years, and to distinguish the sources and control factors of different heavy metals. The sediment quality was also discussed by using the threshold effect concentration (TEC; below which adverse effects are not expected to occur) and the Probable effect concentration (PEC; above which adverse effects are expected to occur more often than not) (MacDonald et al., 2000). This study is important in understanding the long-term evolution and mechanism of atmospheric heavy metal pollution in southern China, which will provide a scientific basis for formulating reasonable strategies in pollution control.

2. Materials and methods

2.1. Study site and sampling

Huguangyan Maar Lake (21°9'N, 110°17'E) is located in Zhanjiang in the northern Leizhou peninsula of Guangdong Province in southern China. The lake was formed by a flat volcanic eruption 160,000 years ago and enclosed by pyroclastic basalt rock walls (Fig. 1). The lake is approximately 2.25 km², with an average depth of 12 m, and a maximum depth of 22 m. There are no river flows into or out of the lake (Chu et al., 2002). The vegetation around the lake is mainly semi-evergreen seasonal forest. The area is strongly affected by the El Niño–Southern Oscillation (ENSO) and tropical cyclones, as well as the joint effects of East Asian and Indian monsoons (Jia et al., 2015).

On August 10, 2020, a 78 cm long sediment core was extracted from the lake center by a gravity sampler, showing a clear sediment–water interface. The sediment core was sectioned at 1.0-cm intervals, and the samples were sealed and stored in 50 mL centrifuge tubes and transported to the laboratory in a refrigerated and airtight container. The samples were freeze-dried at −80 °C, and ground to powder smaller than 63 μm, then stored at −4 °C before chemical analysis.

2.2. Determination of chronology

The activities of ^{210}Pb , ^{226}Ra , and ^{137}Cs were tested using a multi-channel spectrometer (GX6020, Canberra, USA) at the State Key Laboratory of Environmental Geochemistry, Institute of Geochemistry, Chinese Academy of Sciences. The activity of ^{210}Pb was determined by γ -ray at 46.5

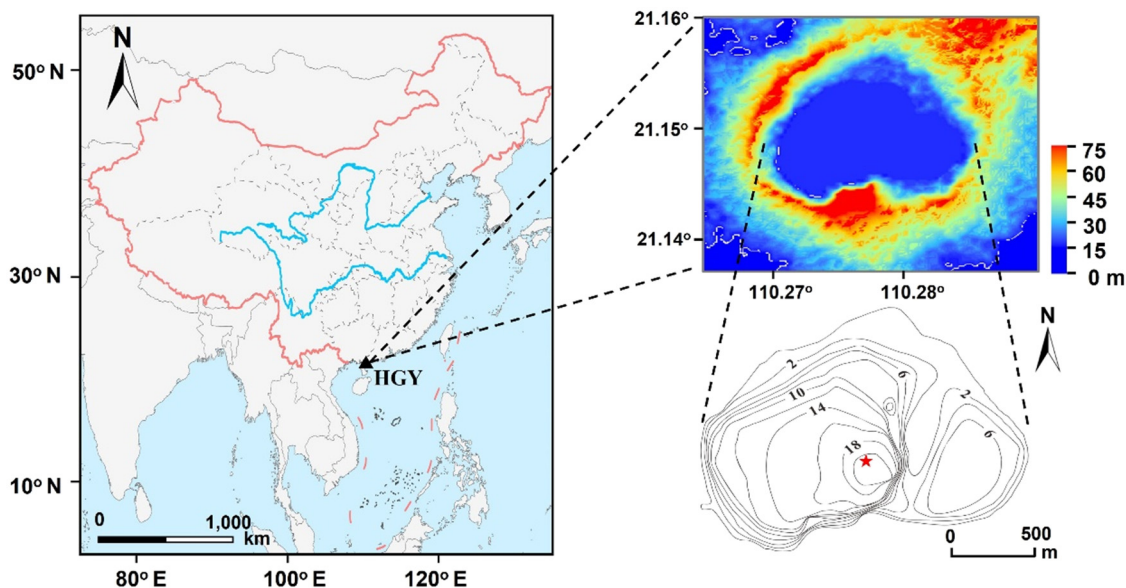


Fig. 1. Map of the study area and location of the sampling site.

keV, the activity of ^{137}Cs was determined by γ -ray at 662 keV, and the activity of ^{226}Ra was determined by γ -ray emitted by its progeny isotope ^{214}Pb at 295 keV and 352 keV. The excess activity of ^{210}Pb ($^{210}\text{Pb}_{\text{ex}}$) was calculated by subtracting the activity of ^{226}Ra from the measured activity of ^{210}Pb . The absolute efficiency of the detector was determined using a calibrated source and a sediment sample with known activity. The self-absorption effect of low-energy γ -ray inside the sample has been corrected. The Constant Flux and Constant Sedimentation Rate (CFCS) model was utilized to evaluate the chronology, and the dry bulk density was measured by dividing dry weight by volume. Instead of depth, mass depth was used to calculate the sediment accumulation rate because the sediment is usually compacted in the lower part of the sediment core. Mass depth $M(x)$ at depth x is calculated using the formula:

$$M(x) = \int_0^x \rho(s) ds \quad (1)$$

where $\rho(s)$ is the dry bulk density at depth s .

2.3. Geochemistry analysis

To determine the concentrations of main and trace elements in the sediment, 50 mg of sample was weighed and then digested in an HNO_3 and HF system at 180 °C for 48 h. After evaporation, the samples were redissolved in diluted HNO_3 and an inductive-coupled plasma optical emission spectrometer (ICP-AES, Vista-MPX, Varian, USA) was used to determine the concentrations of major elements and inductively coupled plasma mass spectrometry (ICP-MS; 7700 ×, Agilent, USA) was used to determine the concentrations of trace elements. Quality control was performed using blank samples and standard reference material (GBW07407). A set of parallel samples for every 10 samples was measured ($n = 3$). The recovery rate of all elements was within 90–110%. Repeated analysis showed that the relative standard deviation (RSD) of most elements was less than 5% except for Cd (<14%) and Sb (<15%).

The $^{208}\text{Pb}/^{206}\text{Pb}$ and $^{206}\text{Pb}/^{207}\text{Pb}$ of the samples were determined with a multi-receiver inductance-coupled plasma mass spectrometer (Nu Plasma II, Thermo Fisher Scientific, USA). Each ground sample (0.1–0.3 g) was digested with HCl, HNO_3 , and HF. Anion exchange resin (Dowex-1 × 8) was used to extract Pb from the digestion solution and Tl was added before the measurement to enhance the accuracy (Reuer et al., 2003). All acids used in the experiment were prepared through a secondary distillation, except HBr, which was prepared by applying anion exchange resin (Dowex-1 × 8) to purify. The above steps were all completed in a class 1000 clean room. A parallel sample determination was performed for every 10 samples, and an international standard reference material (NIST-SRM981) was used for quality control, inserted before and after the sample measurement, and for every five samples. The relative deviations of the measured $^{208}\text{Pb}/^{206}\text{Pb}$ and $^{206}\text{Pb}/^{207}\text{Pb}$ with respect to NIST-SRM981 standard value were all less than 0.1%, and the parallel relative deviations of $^{208}\text{Pb}/^{206}\text{Pb}$ and $^{206}\text{Pb}/^{207}\text{Pb}$ were less than 0.1% and 0.15%, respectively.

2.4. Data analysis

Principal component analysis (PCA) was used to explore the correlation between elements, using SPSS 21.0 (SPSS Inc., USA). Through the maximum variance method for rotation, only the principal component axis with the eigenvalue greater than 1 is retained. Before analysis, concentration data was normalized in the form of the centralized logarithmic ratio to eliminate differences in the concentration magnitudes among the elements. The flux of heavy metal was calculated by multiplying concentration by sediment accumulation rate. The Enrichment factor (EF) was adopted to evaluate the degree of pollution from heavy metals, with the following calculation formula (Reimann and de Caritat, 2005):

$$EF = (M/R)_s / (M/R)_b \quad (2)$$

where M denotes the target element concentration; s and b denote the sample and background, respectively; and R denotes the reference element concentration, usually with rock-forming elements such as Al, Fe, and Ti selected. Fe was selected in this study. The element concentration at the bottom of the sediment core (> 47 cm) was selected as the background value.

The three-end-member model was used to calculate the proportions of Pb contributed by natural sources, coal combustion, and vehicle exhaust emission, respectively (Li et al., 2011). The calculation formulas were as follows:

$$f_1 + f_2 + f_3 = 1 \quad (3)$$

$$(f_1 \times C_s) / C_1 + (f_2 \times C_s) / C_2 + (f_3 \times C_s) / C_3 = 1 \quad (4)$$

$$f_1 \times R_1 + f_2 \times R_2 + f_3 \times R_3 = R_s \quad (5)$$

where, f_1 , f_2 , and f_3 denote the contribution proportions of natural source, coal combustion, and vehicle exhaust emission, respectively; C_1 , C_2 , C_3 , and C_s denote the Pb concentrations in natural source, coal combustion dust, vehicle exhaust dust, and the sample, respectively (Chen et al., 2005; Tan et al., 2006); and R_1 , R_2 , R_3 , and R_s denote the $^{207}\text{Pb}/^{206}\text{Pb}$ ratios of natural source, coal combustion dust, vehicle exhaust dust, and the sample, respectively (Chen et al., 2005; Tan et al., 2006).

Data analysis was performed using Excel and SPSS 21.0, and graphs were drawn using ArcGis 10.7 (ESRI, USA) and Origin 18.0 (OriginLab, USA).

3. Results and discussion

3.1. Radioisotope chronology and sediment rate

Variation trends in the activity of $^{210}\text{Pb}_{\text{ex}}$ and ^{137}Cs are shown in Fig. 2. The activity of $^{210}\text{Pb}_{\text{ex}}$ shows an exponential decay trend ($R^2 = 0.9539$) with increasing mass depth. Considering relatively greater uncertainties of $^{210}\text{Pb}_{\text{ex}}$ in the lower core section, data above 30 cm was used to calculate the sediment accumulation rate. Although there is dating uncertainty in the lower part of the core, it likely has little influence on drawing main conclusions because in the sediment core, the changes in heavy metals occurred mainly in the upper part. The CFCS model shows that the sediment accumulation rate in Huguangyan Maar Lake is approximately 0.0576 g/($\text{cm}^2 \cdot \text{a}$) (Appleby and Oldfield, 1978). The mass depth of 3.36 g/ cm^2 (depth of 23 cm) corresponds to the year 1963, which is consistent with the peak of ^{137}Cs . Since changes in atmospheric heavy metals caused by anthropogenic activities mainly occur after the Industrial Revolution, the heavy metal concentrations at the bottom of the sediment core (> 47 cm) was selected to reflect natural background information before the Industrial Revolution.

3.2. Historical trends of metal elements

PCA was used to determine the correlation between hazardous heavy metals elements and other major elements in the sediment core. Two principal components with eigenvalue greater than 1 were extracted, which can explain 78.64% of the data variability (Fig. 3). According to the PCA results, metal elements can be divided into three groups. The first group includes Zn, Cd, Sb, Tl, and Pb, which have high strong positive correlations with PC1. These elements are all typical pollution elements caused by anthropogenic activities (Cheng et al., 2015; Zhang et al., 2018). The second group includes alkaline metal elements such as Sr, Na, Ca, Ba, which have strong positive correlations with PC2. The precipitation and dissolution of these elements are greatly affected by aquatic environmental conditions and processes after the deposition stage. The elements of third group have negative correlations with PC1 and PC2. In addition to the two heavy metal elements of Cr and Ni, the third group also includes lithogenic elements such as Fe, Zr, and Ga (Corella et al., 2021; Li et al., 2017). Therefore,

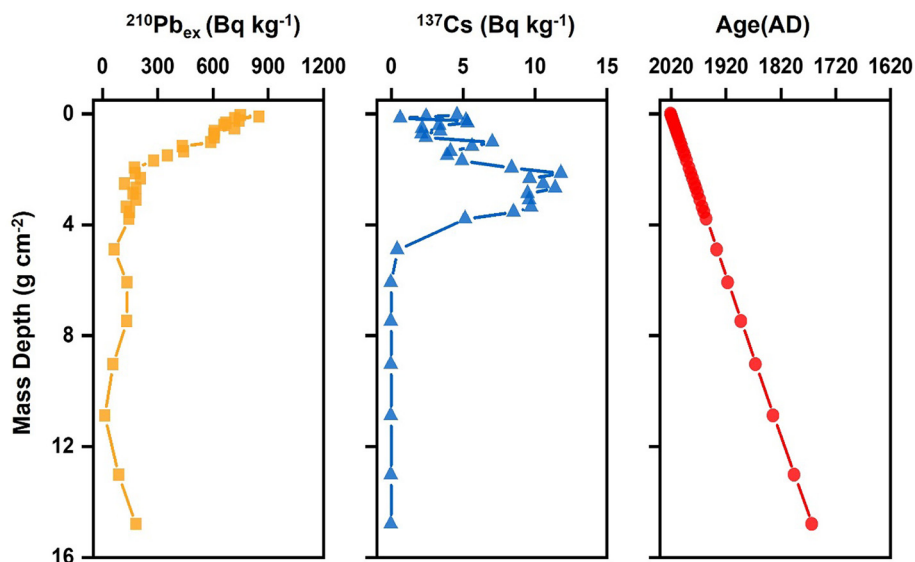


Fig. 2. $^{210}\text{Pb}_{\text{ex}}$, ^{137}Cs activity-mass depth profiles and the chronology in the sediment core of Huguangyan Maar Lake.

the two heavy metal elements of Cr and Ni may mainly come from debris particles produced by rock weathering.

The variations in heavy metal fluxes and EF values in the sediment core are shown in Fig. 4. The variation characteristics of Zn, Cd, Sb, and Tl are similar, consistent with the PCA analysis results. Before and after the Industrial Revolution (1850), the fluxes of Zn, Cd, Sb, and Tl were relatively stable and similar to background levels. Compared with those before the Industrial Revolution, the average Zn flux did not increase between 1850 and 1980, while the Cd flux only increased by 8.5%, Sb increased by 91.6%, and Tl increased by 5.4%. However, the fluxes of Zn, Cd, Sb, and Tl all increased rapidly after 1980. During 1980–2019, the fluxes of Zn, Cd, Sb and Tl ranged from 7.521 to $10.806 \mu\text{g cm}^{-2} \text{yr}^{-1}$, 0.012 to $0.051 \mu\text{g cm}^{-2} \text{yr}^{-1}$, 0.024 to $0.160 \mu\text{g cm}^{-2} \text{yr}^{-1}$ and 0.015 to $0.038 \mu\text{g cm}^{-2} \text{yr}^{-1}$, respectively. After 1980, their average fluxes are increased by 12.1%, 145.9%, 1290.7%, and 113.2%, respectively, compared with those before the Industrial Revolution. The EF values of Zn, Sb, Cd, and Tl also increased significantly, with maximum values of 2.23, 29.32, 5.0, and 3.5, respectively. Industrial activities, such as ore smelting and coal combustion, are the main factors driving the current rise in heavy metal concentrations in environments (Laforte et al., 2005; Li et al., 2017; Sonke et al., 2008; Wan et al., 2016; Xu et al., 2019). Since China implemented the Reform and Opening-

up policy in 1978, the degree of industrialization throughout the country has rapidly increased. Correspondingly, atmospheric concentrations of heavy metals also increased rapidly (Fig. 5) (Tian et al., 2015). The temporal variations of Zn, Sb, Cd, and Tl fluxes in Huguangyan Maar Lake are consistent with the regional industrial development (Fig. 5), indicate that the rise in atmospheric concentrations of these heavy metals may mainly be attribute to the industrial development.

However, Unlike Zn, Cd, Sb, Tl, the fluxes of Cr, and Ni showed decreasing trends after 1980, inconsistent with the trend of atmospheric emissions of Cr and Ni in China or local industrial development (Fig. 5). Compared with the fluxes before the Industrial Revolution, the average fluxes of Fe, Cr, and Ni have decreased by 12.0%, 15.5%, and 10.6% since 1980, respectively. The EF values of Cr and Ni are close to 1 and also show gradually decreasing trends after 1980, indicating that although the concentrations and fluxes of Cr and Ni in Huguangyan Maar Lake sediments are relatively high (Fig. S1, Fig. 4), they mainly derived from natural sources, not anthropogenic activities. Huguangyan lakes are enclosed by basaltic pyroclastic rock, and basalt is mainly composed of mafic silicate minerals (feldspar, pyroxene, olivine, hornblende, and biotite) and glassy matrix, which contain large amounts of Cr, Ni, Zn, and Pb (Chu et al., 2002; Wu et al., 2021). Therefore, Cr and Ni in lake sediments should be mainly derived from the weathering of basalt surrounding the lake.

Atmospheric Pb emissions in China before 1949 were generally thought to be low, and then gradually increased. After 2000, with the complete ban on leaded gasoline, atmospheric emissions of Pb dropped significantly, but then increased again due to coal combustion and fuel consumption (Fig. 5) (Cheng and Hu, 2010; Tian et al., 2015). This trend has been widely recorded by remote mountain lakes in central, north, southwest, and northeast China (Li et al., 2017; Liu et al., 2013a; Pratte et al., 2019; Wan et al., 2020). However, the variations of Pb in Huguangyan sediments indicate that southern China may have a different history of atmospheric Pb emissions. Pb flux was relatively stable before 1850, then gradually increased after 1850, and reached a maximum of $3.592 \mu\text{g cm}^{-2} \text{yr}^{-1}$ around 1950, showing an increase of 470.7% compared with before the Industrial Revolution. From 1950 to 2000, Pb flux gradually declined, but was still higher than before the Industrial Revolution. After 2000, Pb flux rose again, as did Zn, Cd, Sb, and Tl, and reached a peak again around 2018, with a flux 4.59 times that of before the Industrial Revolution. The EF value of Pb has gradually increased since 1850 and reached a maximum of 6.0 in 1950, then gradually decreased but still was greater than 2.0. After 2000, the EF value of Pb rose again and peaked at 5.3. The high EF value indicates that Pb in Huguangyan Maar Lake sediments is strongly

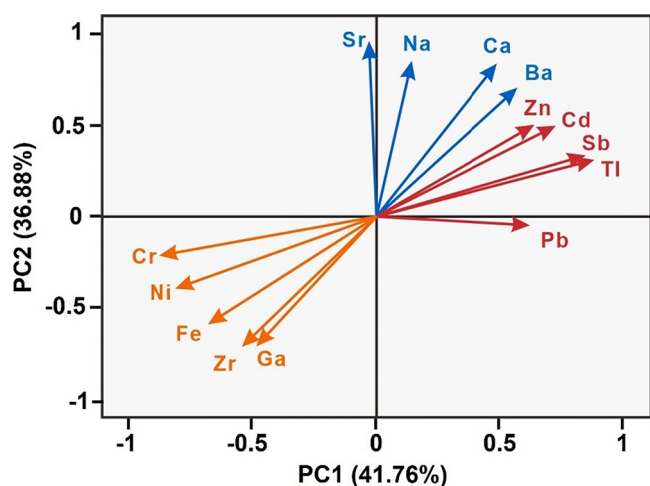


Fig. 3. Loading plots for elements in the sediment core.

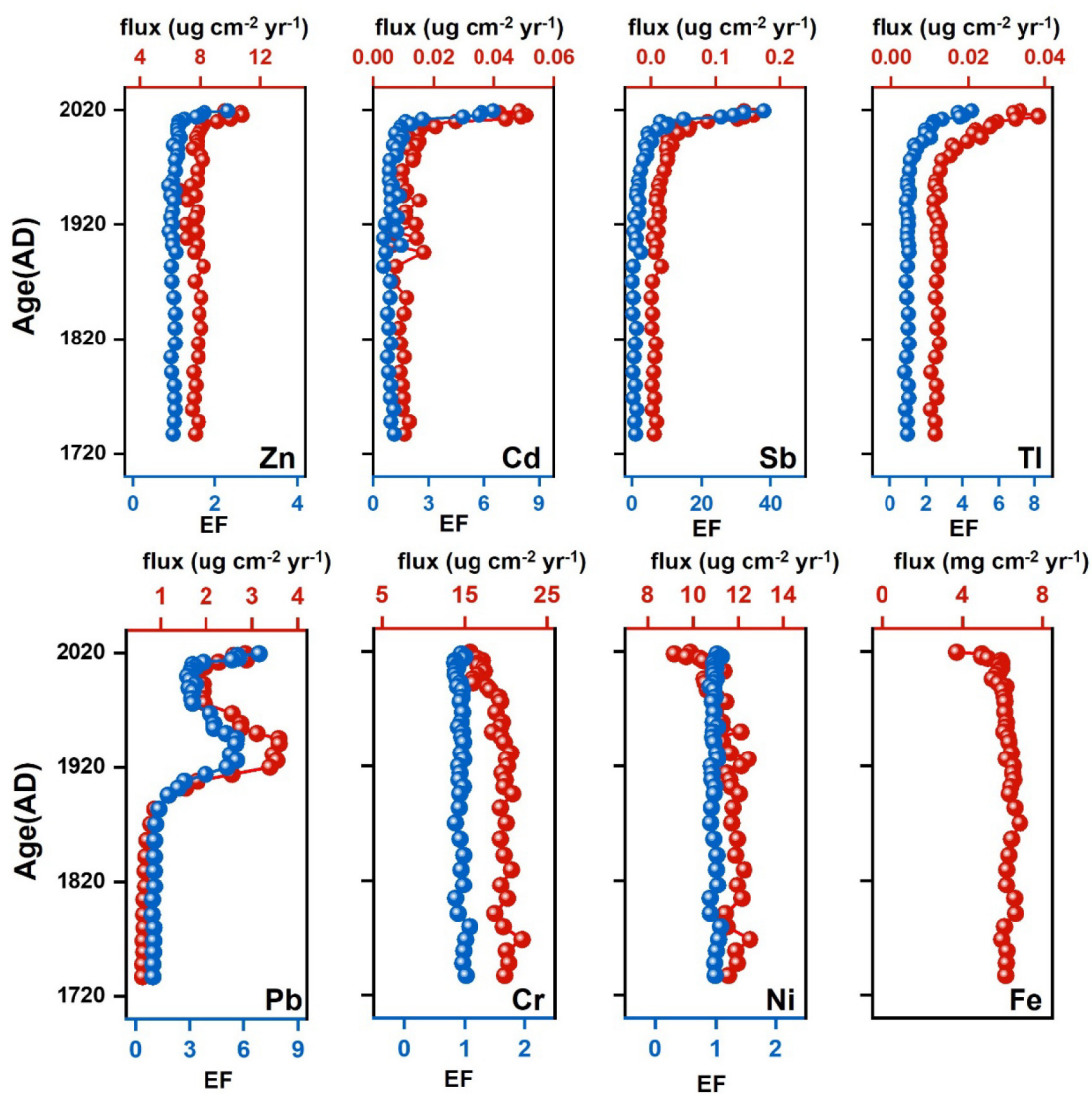


Fig. 4. Temporal variations of metal fluxes (red circle) and EF (blue circle) in the sediment core.

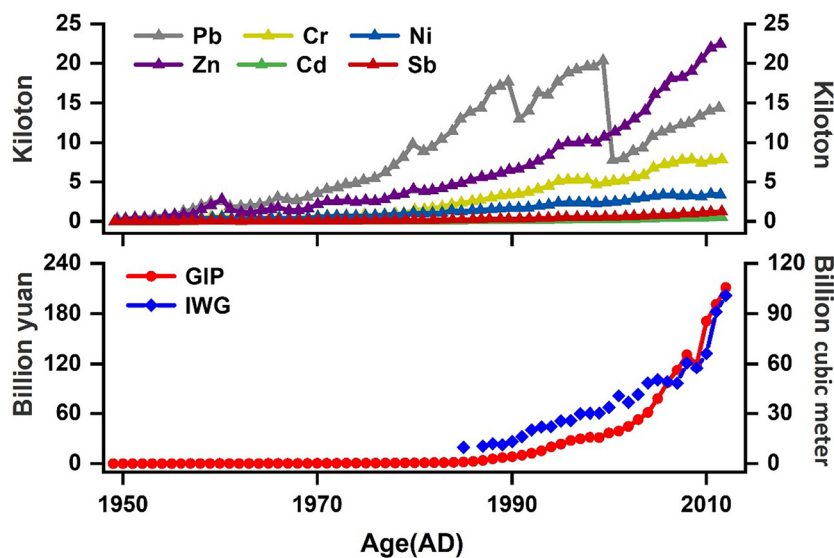


Fig. 5. Estimated atmospheric heavy metal emissions in China (Tian et al., 2015) and gross industrial product (GIP), and industry waste gas (IWG) emissions in Zhanjiang.

affected by anthropogenic activities (Reimann and de Caritat, 2005), while its variation is different from Sb, Cd, and Tl, indicating that Pb may have different anthropogenic activity-affected processes.

Compared with other sedimentary records in China, current fluxes of heavy metals in Huguangyan Maar Lake are higher than those in remote lakes (Li et al., 2021; Wan et al., 2019; Wan et al., 2016), and close to Erhai Lake and Fuxian Lake in Southwest China (Li et al., 2017; Liu et al., 2013b). The heavy metal concentrations in Huguangyan sediments are relatively higher than other lakes in China (Fig.S1). The concentrations of Zn, Cd, Cr, Ni, and Pb in the surface sediments (0–10 cm) exceeds 75% of those in other lakes in China (Cheng et al., 2015; Xu et al., 2017), while the concentrations of Sb and Tl are equivalent to lakes located in large industrial areas such as Taihu Lake and Poyang Lake (Ren et al., 2019; Yu et al., 2012; Zhang et al., 2018). According to the Sediment Quality Guidelines for Freshwater Ecosystems (MacDonald et al., 2000), the concentrations of Zn and Pb in the surface layer of lacustrine sediments exceed the threshold effect concentrations (TEC) but are lower than probable effect concentrations (PEC), while the concentrations of Cr and Ni exceed PEC, indicating these heavy metals may be potentially hazardous to ecosystems.

3.3. Sources of sediment Pb implied by Pb isotopes

Analysis of Pb isotopes indicates that the $^{206}\text{Pb}/^{207}\text{Pb}$ shows an opposite variation trend with Pb flux, while the variation in $^{208}\text{Pb}/^{206}\text{Pb}$ is consistent with the Pb flux (Fig. 6a). Before 1850, $^{206}\text{Pb}/^{207}\text{Pb}$ and $^{208}\text{Pb}/^{206}\text{Pb}$ were relatively stable, with average values of 1.1932 and 2.0831, respectively, which were close to the ratios in natural sources such as loess and sand dust (Fig. 6b) (Ferrat et al., 2012). These results indicate that Pb in lake sediments before 1850 was mainly derived from natural sources. After 1850, $^{206}\text{Pb}/^{207}\text{Pb}$ showed a slight decrease while $^{208}\text{Pb}/^{206}\text{Pb}$ increased slowly. This variation may be related to the development of China's industry when Western countries established numerous factories in China's coastal cities from 1850 to 1910. Within this period, China carried out a series of industrial reforms since 1860, and industries such as textiles, weapons manufacturing, and food processing emerged. Specifically, Guangdong Province is the region where these reforms were first carried out (Lee et al., 2008).

From 1910 to 1950, Pb flux increased rapidly. $^{206}\text{Pb}/^{207}\text{Pb}$ and $^{208}\text{Pb}/^{206}\text{Pb}$ show that the Pb source was strongly affected by anthropogenic activities during this period (Fig. 6b). In this period, frequent wars in southern China may be the main cause for the increase in Pb of sediments as it is one of the main materials to produce firearms and bullets. Analysis of soil in a shooting range shows that Pb concentrations are much higher than

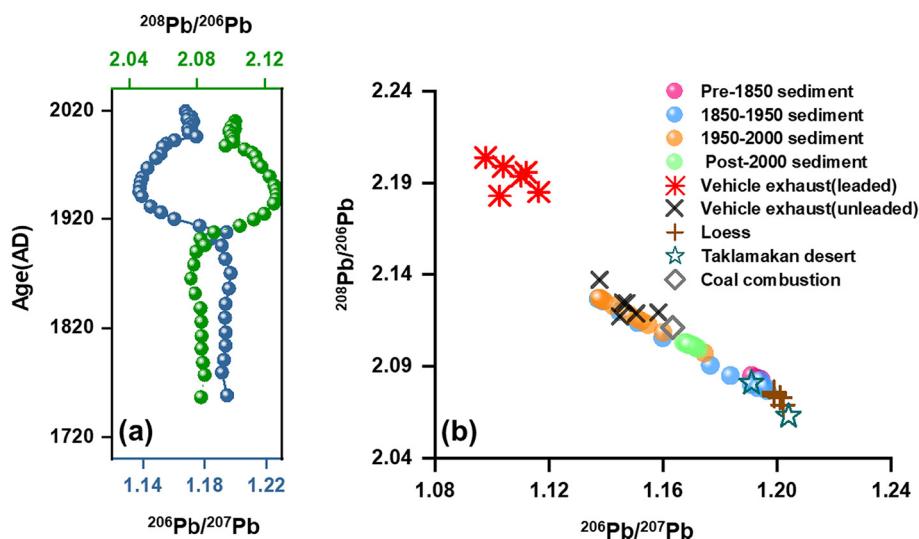


Fig. 6. (a) Plot of $^{206}\text{Pb}/^{207}\text{Pb}$ ratios (blue circle) and $^{208}\text{Pb}/^{206}\text{Pb}$ ratios (green circle) in the sediment core and (b) the values of isotopic ratios of possible Pb emission sources (Chen et al., 2005; Ferrat et al., 2012; Tan et al., 2006) and sediment core.

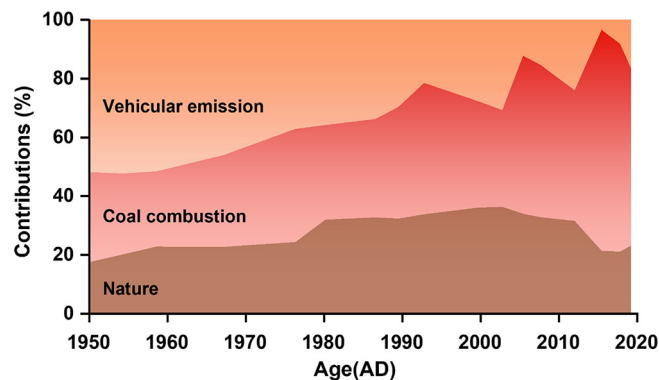


Fig. 7. The proportions of anthropogenic (coal combustion and vehicular emission) and natural Pb sources to total Pb in the sediment core calculated from the three-end-member model of Pb isotopes.

other areas (Fayiga and Saha, 2016). Furthermore, the outbreak of war rapidly intensified military-related industrial manufacturing activities, leading to a rapid increase in atmospheric Pb concentrations (Lee et al., 2008). In addition, the extensive use of leaded gasoline was also an important factor in increasing Pb of sediments during this period (Cheng and Hu, 2010). Since 1921, tetraethyl lead was widely used as an anti-knocking agent added to gasoline, and the amount of leaded gasoline in the world has risen sharply (Nriagu, 1990).

From 1950 to 2000, the social environment stabilized after the founding of the People's Republic of China. The gradual shifts of $^{206}\text{Pb}/^{207}\text{Pb}$ and $^{208}\text{Pb}/^{206}\text{Pb}$, indicate that the input of Pb from anthropogenic activities was gradually decreasing, but still higher than that of natural sources (Fig. 6b). After 2000, $^{206}\text{Pb}/^{207}\text{Pb}$ decreased again while $^{208}\text{Pb}/^{206}\text{Pb}$ increased, which reflects the increase in the Pb input from anthropogenic activities. Although the Chinese government gradually banned the use of leaded gasoline since the 1990s and completely banned leaded gasoline since 2000, the rapid development of industry has continued to increase the atmospheric Pb in southern China (Cheng and Hu, 2010).

Pb proportions derived from different sources after 1950 were calculated according to the three-end-member model (Chen et al., 2005; Li et al., 2011; Tan et al., 2006). The contribution of natural sources to Pb in Huguangyan sediments is ranged from 17% to 35% (Fig. 7). The proportion of Pb derived from vehicle exhaust emissions was highest in the 1960s, reaching more than 50%, and then gradually decreased. Since 2000, as leaded gasoline has been completely banned, Pb from vehicle exhaust gas

has further reduced. Contrary to the variation in the contribution of vehicle exhaust gas emissions, the proportion of Pb derived from coal combustion has gradually increased. After 1980, coal combustion became the main source of Pb, and after 2000, Pb contributed by coal combustion increased rapidly, and accounted for up to 75.4% of the total Pb in 2015 (Fig. 7).

4. Conclusions

Based on isotopic dating using ^{210}Pb and ^{137}Cs , heavy metal concentrations, and Pb isotopes in a sediment core from Huguangyan Maar Lake, the history of atmospheric heavy metal pollution in southern China was reconstructed. The results indicate that Zn, Cd, Sb, and Tl fluxes increased rapidly after 1980, which is consistent with the industrialization process after the Reform and Opening Up. Industrial activities are the main driving factor for the increasing atmospheric concentrations of these heavy metals. The results of PCA and EF (< 2) indicate that Cr and Ni mainly come from the weathering of basalt surrounding the lake, not from anthropogenic activities. Affected by the early modern industrialization in southern China, Pb flux has increased since 1850. During 1910–1950, Pb flux increased rapidly and peaked in 1950 due to the war and the use of leaded gasoline. From 1950 to 2000, Pb flux continuously declined due to the gradual stabilization of the social environment. After 2000, Pb flux rose again with the development of industry. The results of Pb isotopes three end-member model show that in the 1960s, vehicle exhaust contributed the highest proportion of Pb. With the increase in coal consumption and the ban of leaded gasoline, this contribution gradually decreased, while that of coal combustion gradually increased. Nowadays, coal combustion has become the main source of atmospheric Pb. The fluxes of Zn, Cd, Sb, Tl, and Pb of Huguangyan Lake sediments continue to increase with the economic and industrial development of southern China, and the concentrations of most hazardous heavy metals in the surface sediments have exceeded TEC, so monitoring and control measures need to be implemented in this lake. In the aquatic ecosystem, these heavy metals may accumulate or become biomagnified, the subsequent biological effects should be explored in future studies. Affected by temporal and spatial differences in human development, historical atmospheric Pb emissions in southern China are different from those of other regions. Therefore, it is necessary to undertake further studies on the similarities and differences in heavy metal pollution history of different regions.

CRedit authorship contribution statement

Hongchen Wu: Investigation, Formal analysis, Writing - Original Draft, Writing - Review & Editing.

Jingfu Wang: Conceptualization, Methodology, Funding acquisition, Writing - Review & Editing.

Jianyang Guo: Conceptualization, Methodology, Investigation, Formal analysis, Data analysis.

Xinping Hu: Investigation, Formal analysis, Data analysis.

Hongyun Bao: Formal analysis, Data analysis.

Jingan Chen: Supervision, Funding acquisition, Writing - Review & Editing.

Declaration of competing interest

The authors declare that they have no known competing financial interests or personal relationships that could have appeared to influence the work reported in this paper.

Acknowledgements

This study was sponsored jointly by the Strategic Priority Research Program of CAS (No. XDB40020400), the National Key Research and Development Plan of China (2021YFC3201000), the Science and Technology Service Plan of CAS (KFJSTSQYZD202124001), the Chinese NSF project (No. 41773145, 41977296), the Youth Innovation Promotion Association CAS (No. 2019389), and the CAS Interdisciplinary Innovation Team.

Appendix A. Supplementary data

Supplementary data to this article can be found online at <https://doi.org/10.1016/j.scitotenv.2022.154829>.

References

- Appleby, P.G., Oldfield, F., 1978. The calculation of lead-210 dates assuming a constant rate of supply of unsupported ^{210}Pb to the sediment. *Catena* 5, 1–8. [https://doi.org/10.1016/S0341-8162\(78\)80002-2](https://doi.org/10.1016/S0341-8162(78)80002-2).
- Chan, C.K., Yao, X., 2008. Air pollution in mega cities in China. *Atmos. Environ.* 42, 1–42. <https://doi.org/10.1016/j.atmosenv.2007.09.003>.
- Chen, J.M., Tan, M.G., Li, Y.L., Zhang, Y.M., Lu, W.W., Tong, Y.P., Zhang, G.L., Li, Y., 2005. A lead isotope record of shanghai atmospheric lead emissions in total suspended particles during the period of phasing out of leaded gasoline. *Atmos. Environ.* 39, 1245–1253. <https://doi.org/10.1016/j.atmosenv.2004.10.041>.
- Cheng, H., Hu, Y., 2010. Lead (Pb) isotopic fingerprinting and its applications in lead pollution studies in China: a review. *Environ. Pollut.* 158, 1134–1146. <https://doi.org/10.1016/j.envpol.2009.12.028>.
- Cheng, H.X., Li, M., Zhao, C.D., Yang, K., Li, K., Peng, M., Yang, Z.F., Liu, F., Liu, Y.G., Bai, R.J., Cui, Y.J., Huang, Z.F., Li, L.H., Liao, Q.L., Luo, J.L., Jia, S.J., Pang, X.G., Yang, J., Yin, G.S., 2015. Concentrations of toxic metals and ecological risk assessment for sediments of major freshwater lakes in China. *J. Geochem. Explor.* 157, 15–26. <https://doi.org/10.1016/j.gexplo.2015.05.010>.
- Chu, G., Liu, J., Sun, Q., Lu, H., Liu, T., 2002. The 'Mediaeval Warm Period' drought recorded in Lake Huguangyan, tropical South China. *Holocene* 12, 511–516. <https://doi.org/10.1191/0959683602hl566ft>.
- Corella, J.P., Sierra, M.J., Garralon, A., Millan, R., Rodriguez-Alonso, J., Mata, M.P., Vicente de Vera, A., Moreno, A., Gonzalez-Samperiz, P., Duval, B., Amouroux, D., Vivez, P., Cuevas, C.A., Adame, J.A., Wilhelm, B., Saiz-Lopez, A., Valero-Garces, B.L., 2021. Recent and historical pollution legacy in high altitude Lake Marbore (Central Pyrenees): a record of mining and smelting since pre-Roman times in the Iberian Peninsula. *Sci. Total Environ.* 751, 1–16. <https://doi.org/10.1016/j.scitotenv.2020.141557>.
- Fayiga, A.O., Saha, U.K., 2016. Soil pollution at outdoor shooting ranges: health effects, bio-availability and best management practices. *Environ. Pollut.* 216, 135–145. <https://doi.org/10.1016/j.envpol.2016.05.062>.
- Ferrat, M., Weiss, D.J., Dong, S.F., Large, D.J., Spiro, B., Sun, Y.B., Gallagher, K., 2012. Lead atmospheric deposition rates and isotopic trends in Asian dust during the last 9.5 kyr recorded in an ombrotrophic peat bog on the eastern Qinghai-Tibetan Plateau. *Geochim. Cosmochim. Acta* 82, 4–22. <https://doi.org/10.1016/j.gca.2010.10.031>.
- Hall, J.L., 2002. Cellular mechanisms for heavy metal detoxification and tolerance. *J. Exp. Bot.* 53, 1–11. <https://doi.org/10.1093/jxbbot/53.366.1>.
- Huang, J., Kang, S.C., Yin, R.S., Lin, M., Guo, J.M., Ram, K., Li, C.L., Sharma, C., Tripathee, L., Sun, S.W., Wang, F.Y., 2020. Decoupling natural and anthropogenic mercury and lead transport from South Asia to the Himalayas. *Environ. Sci. Technol.* 54, 5429–5436. <https://doi.org/10.1021/acs.est.0c00429>.
- Jia, G., Bai, Y., Yang, X., Xie, L., Wei, G., Ouyang, T., Chu, G., Liu, Z., Peng, P.A., 2015. Biogeochemical evidence of Holocene East Asian summer and winter monsoon variability from a tropical maar lake in southern China. *Quat. Sci. Rev.* 111, 51–61. <https://doi.org/10.1016/j.quascirev.2015.01.002>.
- Kribek, B., Sipkova, A., Ettler, V., Mihaljevic, M., Majer, V., Knesl, I., Mapani, B., Penizek, V., Vanek, A., Sracek, O., 2018. Variability of the copper isotopic composition in soil and grass affected by mining and smelting in Tsumeb, Namibia. *Chem. Geol.* 493, 121–135. <https://doi.org/10.1016/j.chemgeo.2018.05.035>.
- Labonne, M., Ben Othman, D., Luck, J.M., 2001. Pb isotopes in mussels as tracers of metal sources and water movements in a lagoon (Thau Basin, S. France). *Chem. Geol.* 181, 181–191. [https://doi.org/10.1016/S0009-2541\(01\)00281-9](https://doi.org/10.1016/S0009-2541(01)00281-9).
- Laforte, L., Tessier, A., Gobeil, C., Carignan, R., 2005. Thallium diagenesis in lacustrine sediments. *Geochim. Cosmochim. Acta* 69, 5295–5306. <https://doi.org/10.1016/j.gca.2005.06.006>.
- Lee, C.S.L., Qi, S.-H., Zhang, G., Luo, C.-L., Zhao, L.Y.L., Li, X.-D., 2008. Seven thousand years of records on the mining and utilization of metals from lake sediments in central China. *Environ. Sci. Technol.* 42, 4732–4738. <https://doi.org/10.1021/es702990n>.
- Lee, K., Do Hur, S., Hou, S., Burn-Nunes, L.J., Hong, S., Barbante, C., Boutron, C.F., Rosman, K.J.R., 2011. Isotopic signatures for natural versus anthropogenic Pb in high-altitude Mt. Everest ice cores during the past 800 years. *Sci. Total Environ.* 412, 194–202. <https://doi.org/10.1016/j.scitotenv.2011.10.002>.
- Li, S.Y., Sun, W.W., Chen, R., Zhang, Z.J., Ning, D.L., Ni, Z.Y., 2021. A historical record of trace metal deposition in northeastern Qinghai-Tibetan Plateau for the last two centuries. *Environ. Sci. Pollut. Res.* <https://doi.org/10.1007/s11356-021-17618-9>.
- Li, H.-B., Yu, S., Li, G.-L., Deng, H., Luo, X.-S., 2011. Contamination and source differentiation of Pb in park soils along an urban-rural gradient in Shanghai. *Environ. Pollut.* 159, 3536–3544. <https://doi.org/10.1016/j.envpol.2011.08.013>.
- Li, K., Liu, E., Zhang, E., Li, Y., Shen, J., Liuc, X., 2017. Historical variations of atmospheric trace metal pollution in Southwest China: reconstruction from a 150-year lacustrine sediment record in the Erhai Lake. *J. Geochem. Explor.* 172, 62–70. <https://doi.org/10.1016/j.gexplo.2016.10.009>.
- Li, Y.P., Zhang, Z.S., Liu, H.F., Zhou, H., Fan, Z.Y., Lin, M., Wu, D.L., Xia, B.C., 2016. Characteristics, sources and health risk assessment of toxic heavy metals in PM_{2.5} at a megacity of southwest China. *Environ. Geochem. Health* 38, 353–362. <https://doi.org/10.1007/s10653-015-9722-z>.
- Lin, Q., Liu, E., Zhang, E., Nath, B., Shen, J., Yuan, H., Wang, R., 2018. Reconstruction of atmospheric trace metals pollution in Southwest China using sediments from a large and

- deep alpine lake: historical trends, sources and sediment focusing. *Sci. Total Environ.* 613, 331–341. <https://doi.org/10.1016/j.scitotenv.2017.09.073>.
- Liu, E., Zhang, E., Li, K., Nath, B., Li, Y., Shen, J., 2013a. Historical reconstruction of atmospheric lead pollution in central Yunnan province, southwest China: an analysis based on lacustrine sedimentary records. *Environ. Sci. Pollut. Res.* 20, 8739–8750. <https://doi.org/10.1007/s11356-013-1861-0>.
- Liu, E.F., Zhang, E.L., Li, K., Nath, B., Li, Y.L., Shen, J., 2013b. Historical reconstruction of atmospheric lead pollution in central Yunnan province, southwest China: an analysis based on lacustrine sedimentary records. *Environ. Sci. Pollut. Res.* 20, 8739–8750. <https://doi.org/10.1007/s11356-013-1861-0>.
- Liu, Y.H., Liao, W.Y., Li, L., Huang, Y.T., Xu, W.J., 2017. Vehicle emission trends in China's Guangdong Province from 1994 to 2014. *Sci. Total Environ.* 586, 512–521. <https://doi.org/10.1016/j.scitotenv.2017.01.215>.
- Luo, C.L., Liu, C.P., Wang, Y., Liu, X.A., Li, F.B., Zhang, G., Li, X.D., 2011. Heavy metal contamination in soils and vegetables near an e-waste processing site, south China. *J. Hazard. Mater.* 186, 481–490. <https://doi.org/10.1016/j.jhazmat.2010.11.024>.
- MacDonald, D.D., Ingersoll, C.G., Berger, T.A., 2000. Development and evaluation of consensus-based sediment quality guidelines for freshwater ecosystems. *Arch. Environ. Contam. Toxicol.* 39, 20–31. <https://doi.org/10.1007/s002440010075>.
- Nagajyoti, P.C., Lee, K.D., Sreekanth, T.V.M., 2010. Heavy metals, occurrence and toxicity for plants: a review. *Environ. Chem. Lett.* 8, 199–216. <https://doi.org/10.1007/s10311-010-0297-8>.
- Nriagu, J.O., 1990. The rise and fall of leaded gasoline. *Sci. Total Environ.* 92, 13–28.
- Omrani, M., Ruban, V., Ruban, G., Lamprea, K., 2017. Assessment of atmospheric trace metal deposition in urban environments using direct and indirect measurement methodology and contributions from wet and dry depositions. *Atmos. Environ.* 168, 101–111. <https://doi.org/10.1016/j.atmosenv.2017.08.064>.
- Ortiz, J.E., Moreno, L., Torres, T., Vegas, J., Ruiz-Zapata, B., Garcia-Cortes, A., Galan, L., Perez-Gonzalez, A., 2013. A 220 ka palaeoenvironmental reconstruction of the fuentillejo maar lake record (Central Spain) using biomarker analysis. *Org. Geochem.* 55, 85–97. <https://doi.org/10.1016/j.orggeochem.2012.11.012>.
- Pratte, S., Bao, K., Shen, J., De Vleeschouwer, F., Le Roux, G., 2019. Centennial records of cadmium and lead in NE China lake sediments. *Sci. Total Environ.* 657, 548–557. <https://doi.org/10.1016/j.scitotenv.2018.11.407>.
- Pratte, S., Bao, K., Shen, J., Mackenzie, L., Klamt, A.-M., Wang, G., Xing, W., 2018. Recent atmospheric metal deposition in peatlands of northeast China: a review. *Sci. Total Environ.* 626, 1284–1294. <https://doi.org/10.1016/j.scitotenv.2018.01.183>.
- Reimann, C., de Caritat, P., 2005. Distinguishing between natural and anthropogenic sources for elements in the environment: regional geochemical surveys versus enrichment factors. *Sci. Total Environ.* 337, 91–107. <https://doi.org/10.1016/j.scitotenv.2004.06.011>.
- Ren, M.Y., Wang, D., Ding, S.M., Yang, L.Y., Xu, S.W., Yang, C.Y., Wang, Y., Zhang, C.S., 2019. Seasonal mobility of antimony in sediment-water systems in algae- and macrophyte-dominated zones of Lake Taihu (China). *Chemosphere* 223, 108–116. <https://doi.org/10.1016/j.chemosphere.2019.02.013>.
- Reuer, M.K., Boyle, E.A., Grant, B.C., 2003. Lead isotope analysis of marine carbonates and seawater by multiple collector ICP-MS. *Chem. Geol.* 200, 137–153. [https://doi.org/10.1016/s0009-2541\(03\)00186-4](https://doi.org/10.1016/s0009-2541(03)00186-4).
- Rhodes, R.H., Baker, J.A., Millet, M.-A., Bertler, N.A.N., 2011. Experimental investigation of the effects of mineral dust on the reproducibility and accuracy of ice core trace element analyses. *Chem. Geol.* 286, 207–221. <https://doi.org/10.1016/j.chemgeo.2011.05.006>.
- Ruiz-Fernandez, A.C., Hillaire-Marcel, C., Paez-Osuna, F., Ghaleb, B., Caballero, M., 2007. Pb-210 chronology and trace metal geochemistry at Los Tuxtlas, Mexico, as evidenced by a sedimentary record from the Lago Verde crater lake. *Quat. Res.* 67, 181–192. <https://doi.org/10.1016/j.yqres.2006.11.003>.
- Sierra-Hernandez, M.R., Gabrielli, P., Beaudon, E., Wegner, A., Thompson, L.G., 2018. Atmospheric depositions of natural and anthropogenic trace elements on the Guliya ice cap (northwestern Tibetan Plateau) during the last 340 years. *Atmos. Environ.* 176, 91–102. <https://doi.org/10.1016/j.atmosenv.2017.11.040>.
- Sondergaard, J., Asmund, G., Johansen, P., Elberling, B., 2010. Pb isotopes as tracers of mining-related Pb in lichens, seaweed and mussels near a former Pb-Zn mine in West Greenland. *Environ. Pollut.* 158, 1319–1326. <https://doi.org/10.1016/j.envpol.2010.01.006>.
- Sonke, J.E., Sivry, Y., Viers, J., Freydisier, R., Dejonghe, L., Andre, L., Aggarwal, J.K., Fontan, F., Dupre, B., 2008. Historical variations in the isotopic composition of atmospheric zinc deposition from a zinc smelter. *Chem. Geol.* 252, 145–157. <https://doi.org/10.1016/j.chemgeo.2008.02.006>.
- Tan, M.G., Zhang, G.L., Li, X.L., Zhang, Y.X., Yue, W.S., Chen, J.M., Wang, Y.S., Li, A.G., Li, Y., Zhang, Y.M., Shan, Z.C., 2006. Comprehensive study of lead pollution in Shanghai by multiple techniques. *Anal. Chem.* 78, 8044–8050. <https://doi.org/10.1021/ac061365q>.
- Tian, H.Z., Zhu, C.Y., Gao, J.J., Cheng, K., Hao, J.M., Wang, K., Hua, S.B., Wang, Y., Zhou, J.R., 2015. Quantitative assessment of atmospheric emissions of toxic heavy metals from anthropogenic sources in China: historical trend, spatial distribution, uncertainties, and control policies. *Atmos. Chem. Phys.* 15, 10127–10147. <https://doi.org/10.5194/acp-15-10127-2015>.
- Wan, D., Song, L., Mao, X., Yang, J., Jin, Z., Yang, H., 2019. One-century sediment records of heavy metal pollution on the southeast Mongolian Plateau: implications for air pollution trend in China. *Chemosphere* 220, 539–545. <https://doi.org/10.1016/j.chemosphere.2018.12.151>.
- Wan, D., Yang, H., Jin, Z., Xue, B., Song, L., Mao, X., Yang, J., 2020. Spatiotemporal trends of atmospheric Pb over the last century across inland China. *Sci. Total Environ.* 729, 1–11. <https://doi.org/10.1016/j.scitotenv.2020.138399>.
- Wan, D.J., Song, L., Yang, J.S., Jin, Z.D., Zhan, C.L., Mao, X., Liu, D.W., Shao, Y., 2016. Increasing heavy metals in the background atmosphere of central North China since the 1980s: evidence from a 200-year lake sediment record. *Atmos. Environ.* 138, 183–190. <https://doi.org/10.1016/j.atmosenv.2016.05.015>.
- Wang, L., Li, C., Ying, Q., Cheng, X., Wang, X., Li, X., Hu, L., Liang, L., Yu, L., Huang, H., Gong, P., 2012. China's urban expansion from 1990 to 2010 determined with satellite remote sensing. *Chin. Sci. Bull.* 57, 2802–2812. <https://doi.org/10.1007/s11434-012-5235-7>.
- Wiklund, J.A., Kirk, J.L., Muir, D.C.G., Gleason, A., Carrier, J., Yang, F., 2020. Atmospheric trace metal deposition to remote Northwest Ontario, Canada: anthropogenic fluxes and inventories from 1860 to 2010. *Sci. Total Environ.* 749. <https://doi.org/10.1016/j.scitotenv.2020.142276>.
- Wong, S.C., Li, X.D., Zhang, G., Qi, S.H., Min, Y.S., 2002. Heavy metals in agricultural soils of the Pearl River Delta, South China. *Environ. Pollut.* 119, 33–44. [https://doi.org/10.1016/s0269-7491\(01\)00325-6](https://doi.org/10.1016/s0269-7491(01)00325-6).
- Wu, W., Qu, S., Nel, W., Ji, J., 2021. The influence of natural weathering on the behavior of heavy metals in small basaltic watersheds: a comparative study from different regions in China. *Chemosphere* 262, 1–11. <https://doi.org/10.1016/j.chemosphere.2020.127897>.
- Xu, J.-W., Martin, R.V., Henderson, B.H., Meng, J., Oztaner, Y.B., Hand, J.L., Hakami, A., Strum, M., Phillips, S.B., 2019. Simulation of airborne trace metals in fine particulate matter over North America. *Atmos. Environ.* 214. <https://doi.org/10.1016/j.atmosenv.2019.116883>.
- Xu, Y.F., Wu, Y., Han, J.G., Li, P.P., 2017. The current status of heavy metal in lake sediments from China: pollution and ecological risk assessment. *Ecol. Evol.* 7, 5454–5466. <https://doi.org/10.1002/ece3.3124>.
- Yu, T., Zhang, Y., Meng, W., Hu, X.N., 2012. Characterization of heavy metals in water and sediments in Taihu Lake, China. *Environ. Monit. Assess.* 184, 4367–4382. <https://doi.org/10.1007/s10661-011-2270-9>.
- Zhang, H., Wan, Z.W., Ding, M.J., Wang, P., Xu, X.L., Jiang, Y.H., 2018. Inherent bacterial community response to multiple heavy metals in sediment from river-lake systems in the Poyang Lake, China. *Ecotoxicol. Environ. Saf.* 165, 314–324. <https://doi.org/10.1016/j.ecoenv.2018.09.010>.
- Zhang, R., Guan, M.L., Shu, Y.J., Shen, L.Y., Chen, X.X., Zhang, F., Li, T.G., Jiang, T.C., 2016. Reconstruction of historical lead contamination and sources in Lake Hailing, eastern China: a Pb isotope study. *Environ. Sci. Pollut. Res.* 23, 9183–9191. <https://doi.org/10.1007/s11356-016-6166-7>.